Electronic Supplementary Material (ESI) for RSC Advances.

Supporting information for:

Reactions of Nickel Boranyl Compounds with Pnictogen-Carbon Triple Bonds

Brady J. H. Austen, Marissa L. Clapson, and Marcus W. Drover*

*E-mail: marcus.drover@uwindsor.ca

Department of Chemistry and Biochemistry, The University of Windsor, 401 Sunset Avenue, Windsor, ON, N9B 3P4, Canada

Multinuclear NMR Data:

Figure S1. 2, ^{1}H NMR, tol-d$_8$, 500 MHz, 298 K.

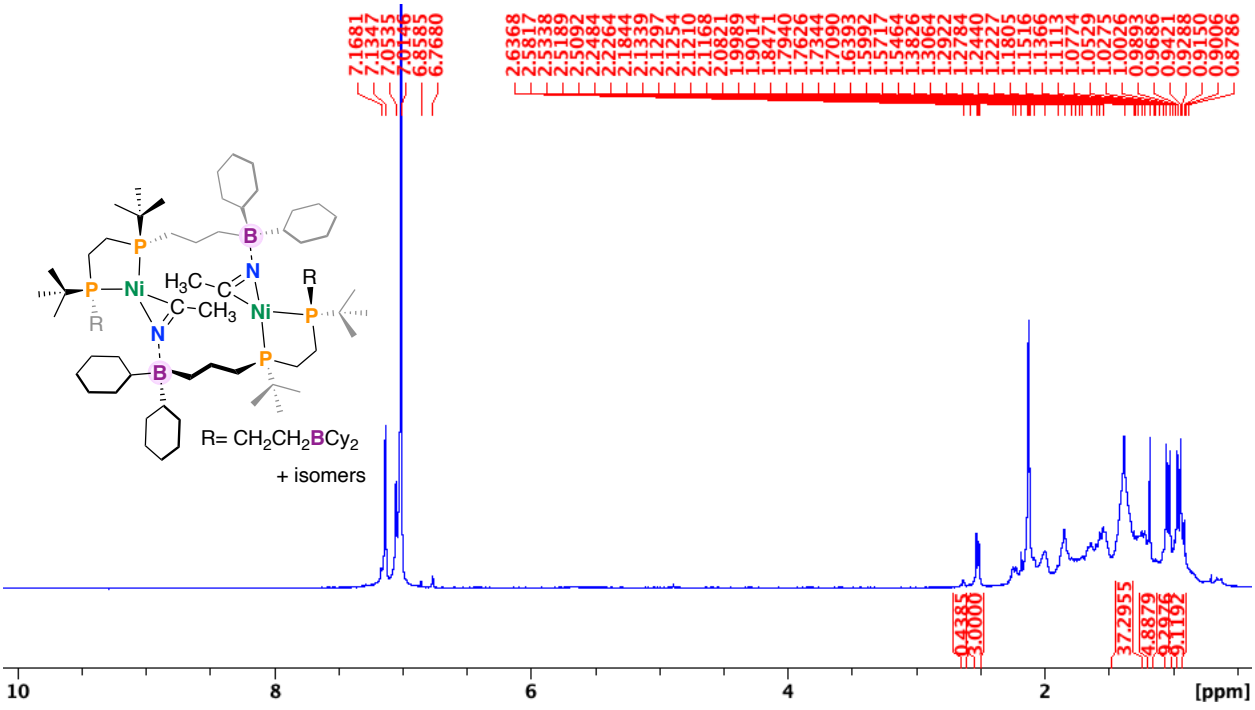

Figure S2. 2, ^{1}H -^{1}H{^{31}P} NMR Overlay, tol-d$_8$, 500 MHz, 298 K.

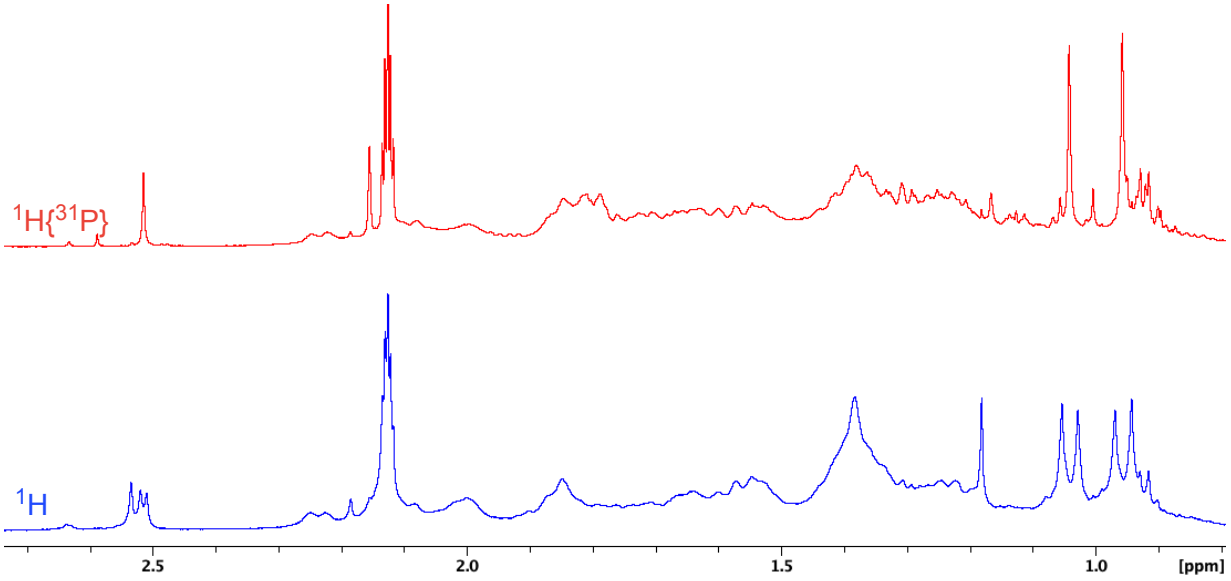

Figure S3. 2, $^{31}P\{^{1}H\}$ NMR, tol-d_8, 203 MHz, 298 K.

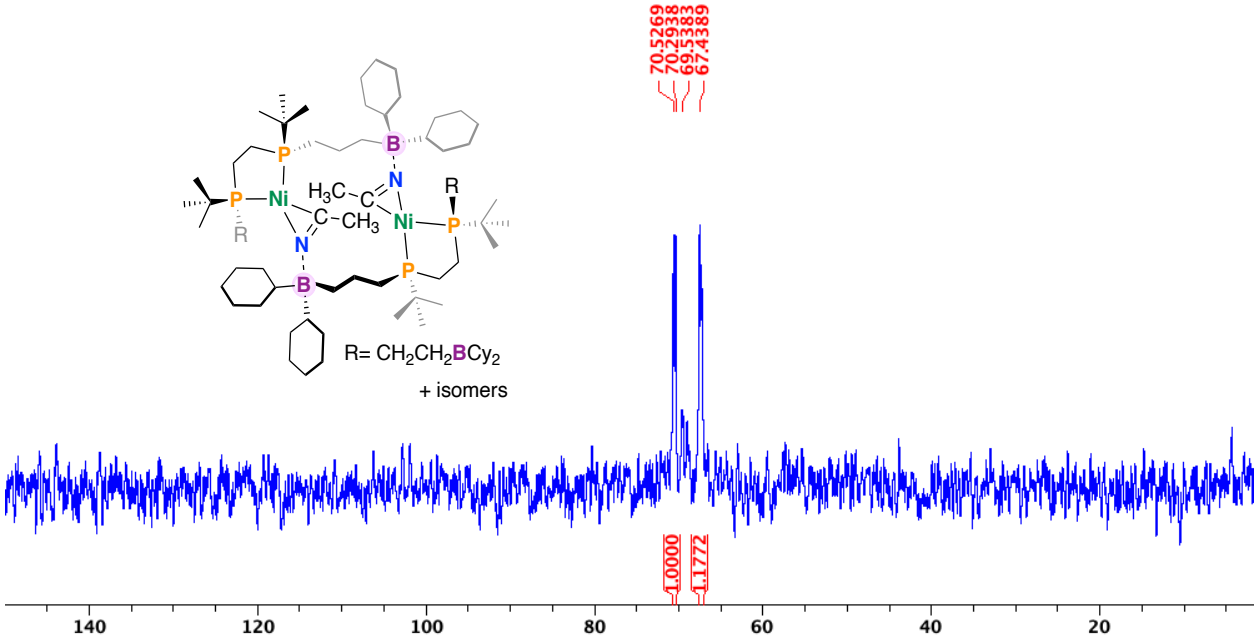

Figure S4. 2, $^{31}P\{^{1}H\}$ NMR expansion, tol-d_8, 203 MHz, 298 K.

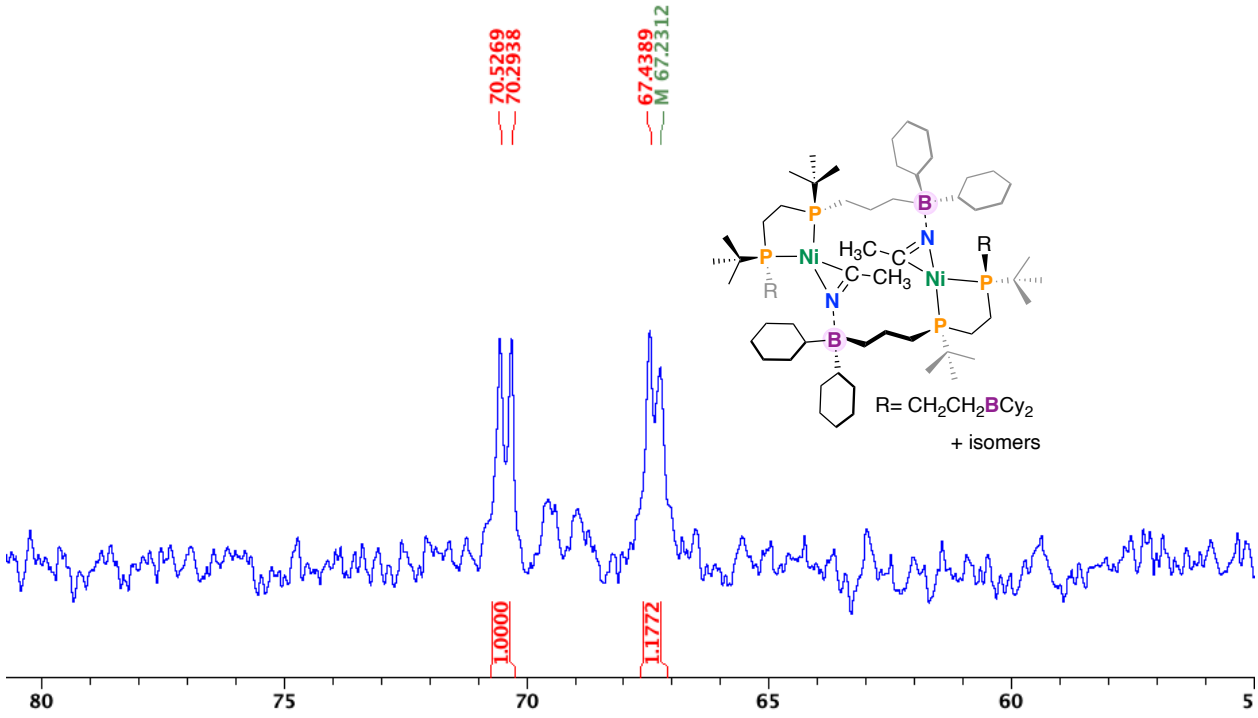

Figure S5. 2, $^{11}B\{^{1}H\}$ NMR, tol-d_8, 96.3 MHz, 298 K, Inset collected at 160.5 MHz.

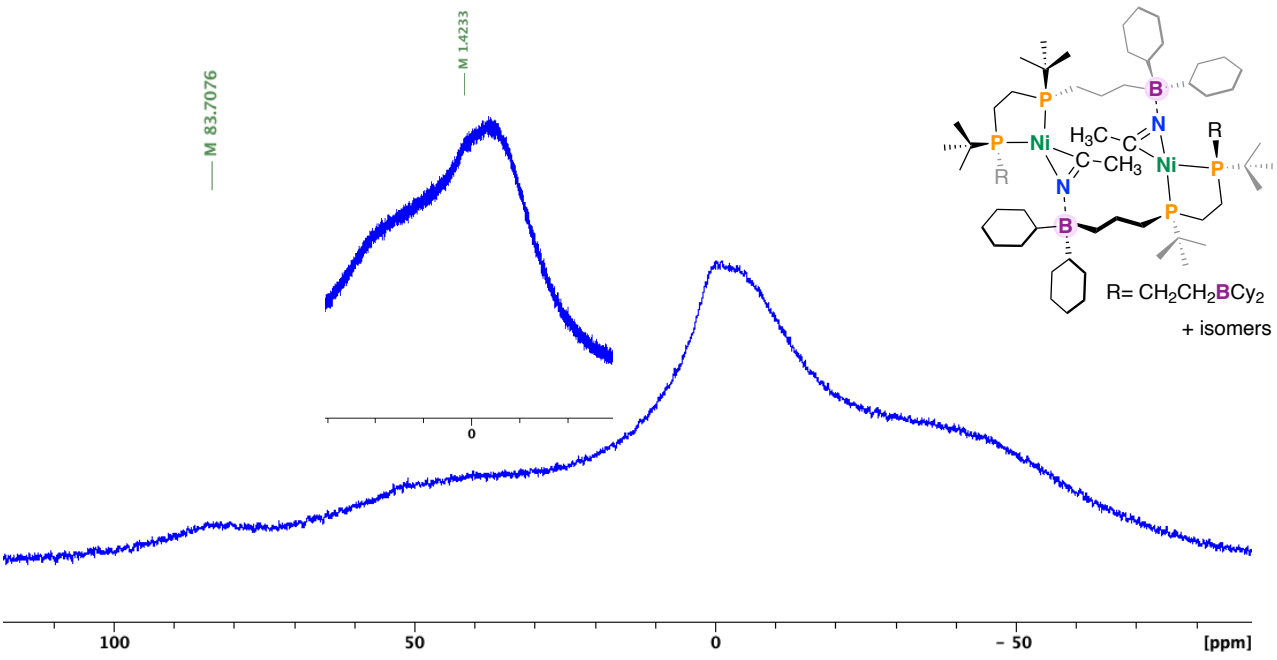

Figure S6. 2, $^{13}C\{^{1}H\}$ NMR, tol-d_8, 125 MHz, 298 K.

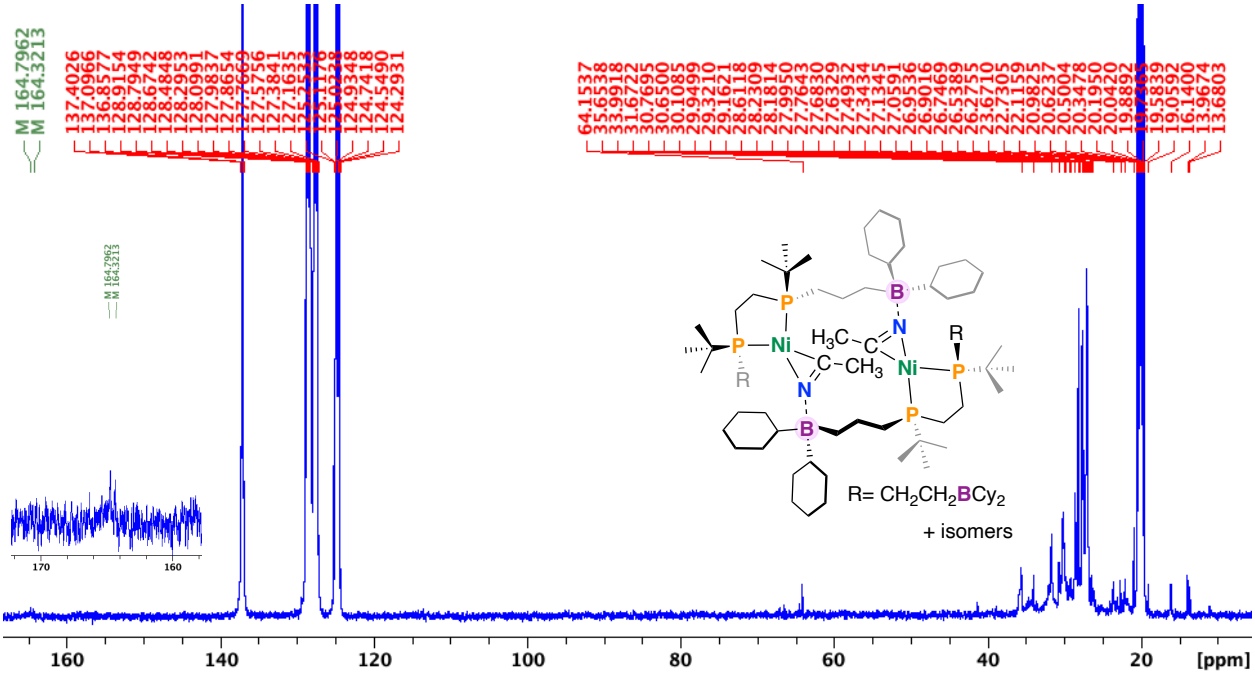

Figure S7. 2, IR Overlay of free CH_3CN and complex **2** comparing υ(CN).

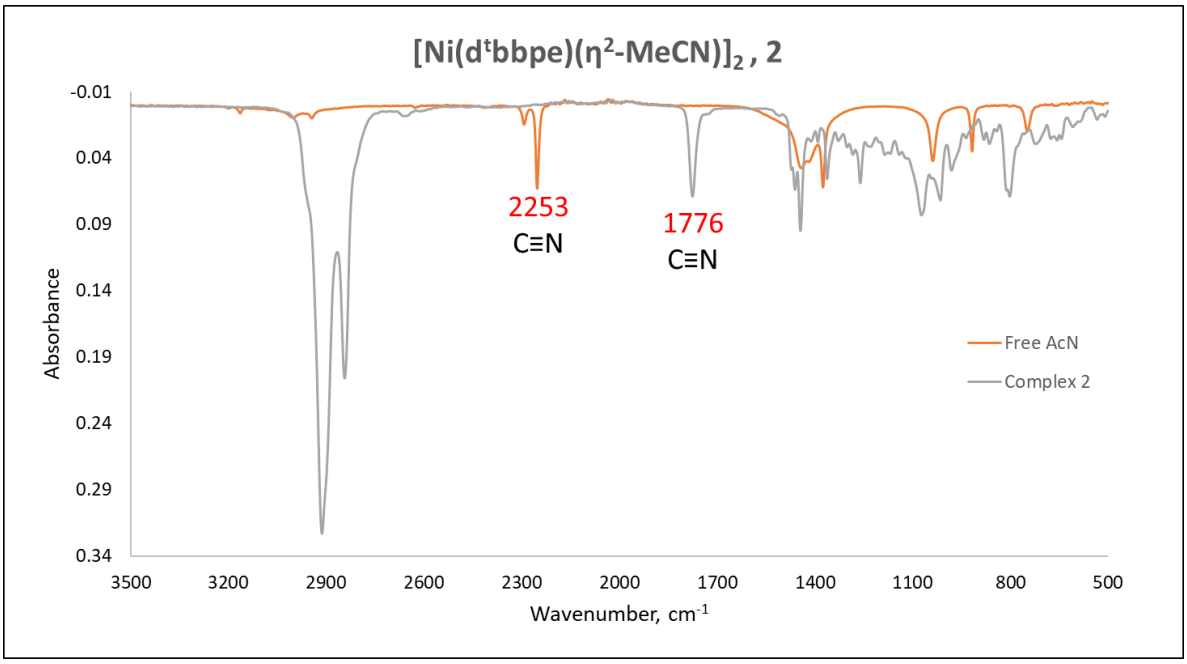

Figure S8. 3, ^1H NMR, tol-d_8, 500 MHz, 298 K.

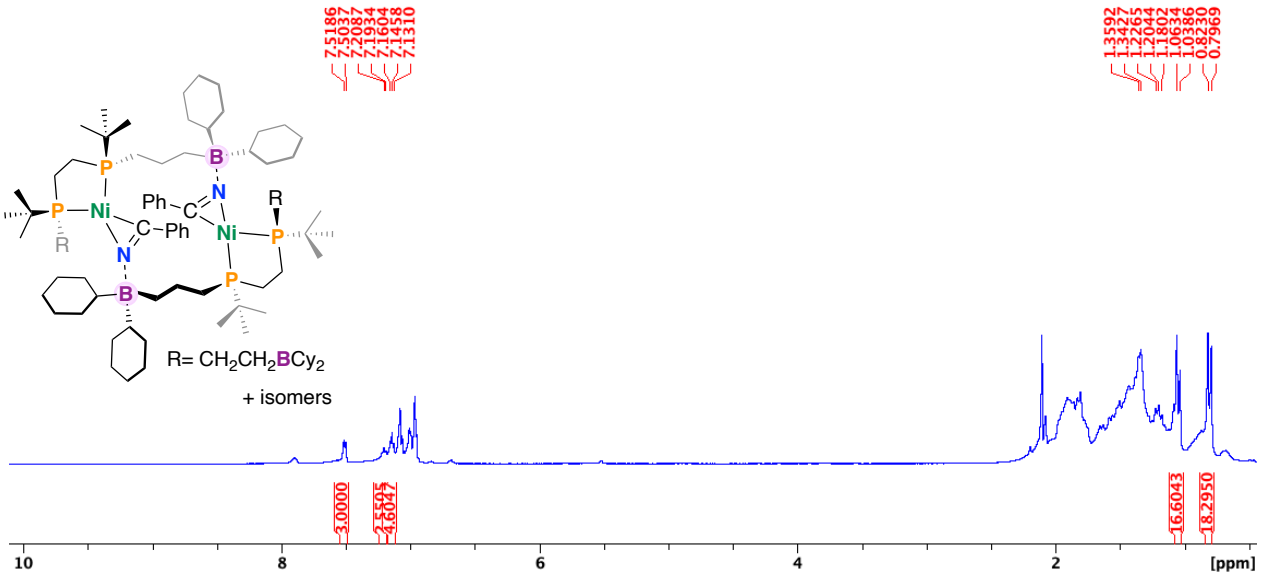

Figure S9. 3, $^{31}P\{^{1}H\}$ NMR, tol-d_8, 203 MHz, 298 K.

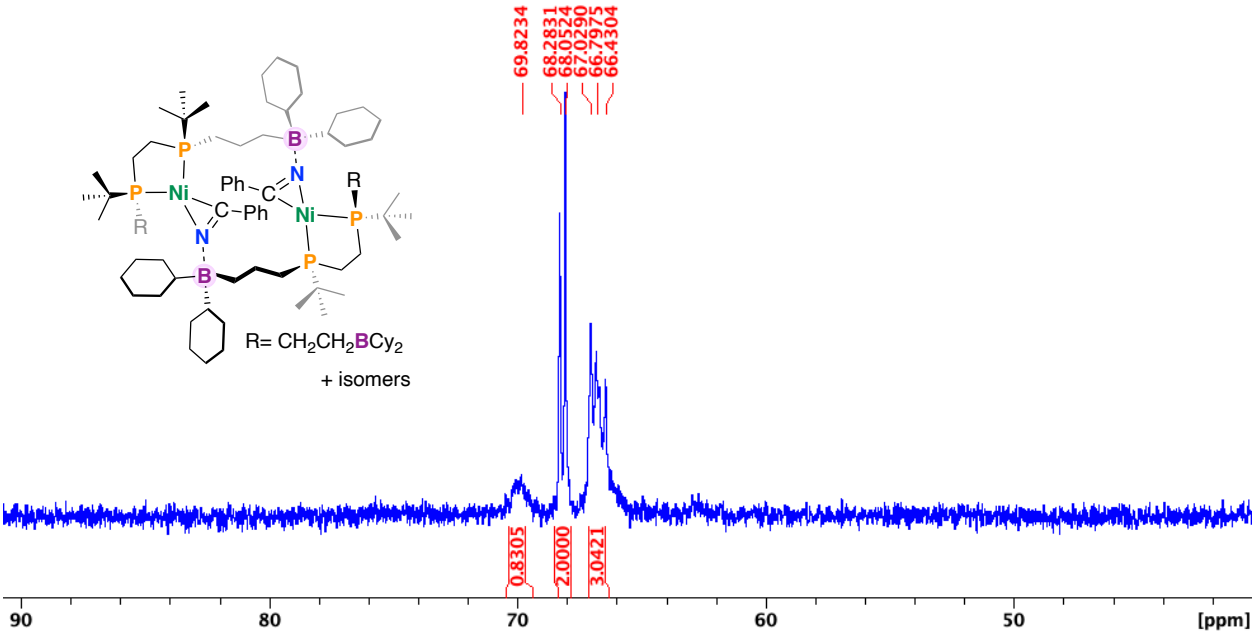

Figure S10. 3, $^{31}P\{^{1}H\}$ NMR Expansion, tol-d_8, 203 MHz, 298 K.

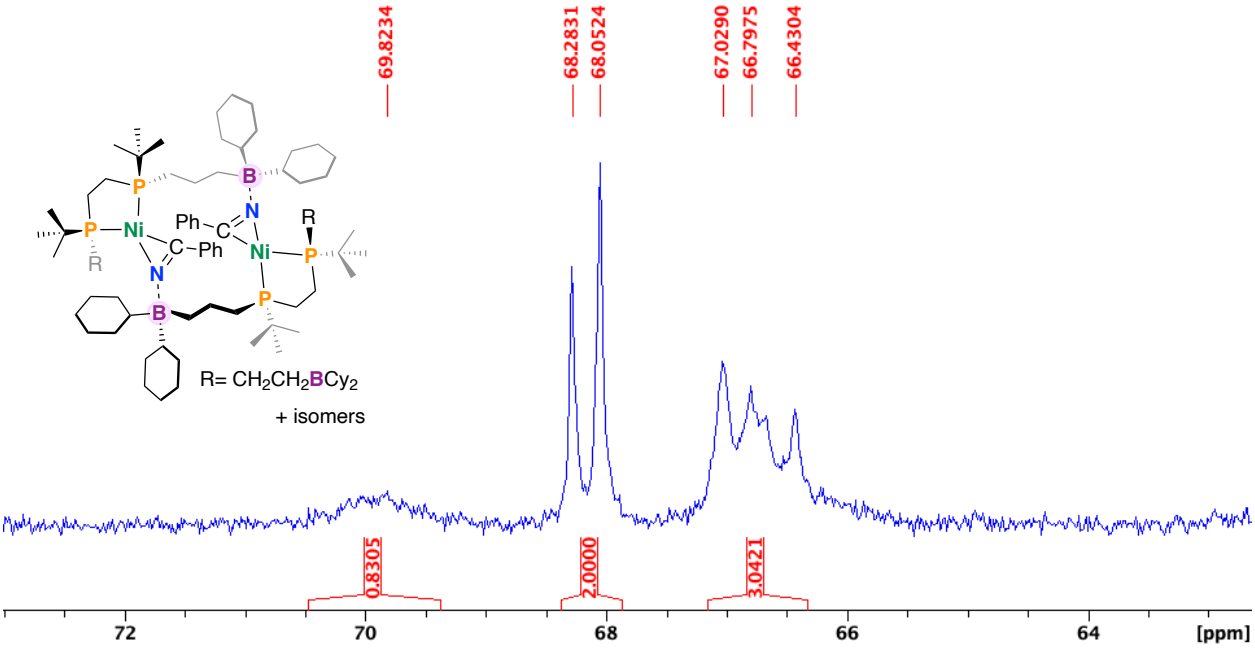

Figure S11. 3, $^{11}B\{^{1}H\}$ NMR, tol-d_8, 96.3 MHz, 298 K, Inset collected at 160.5 MHz.

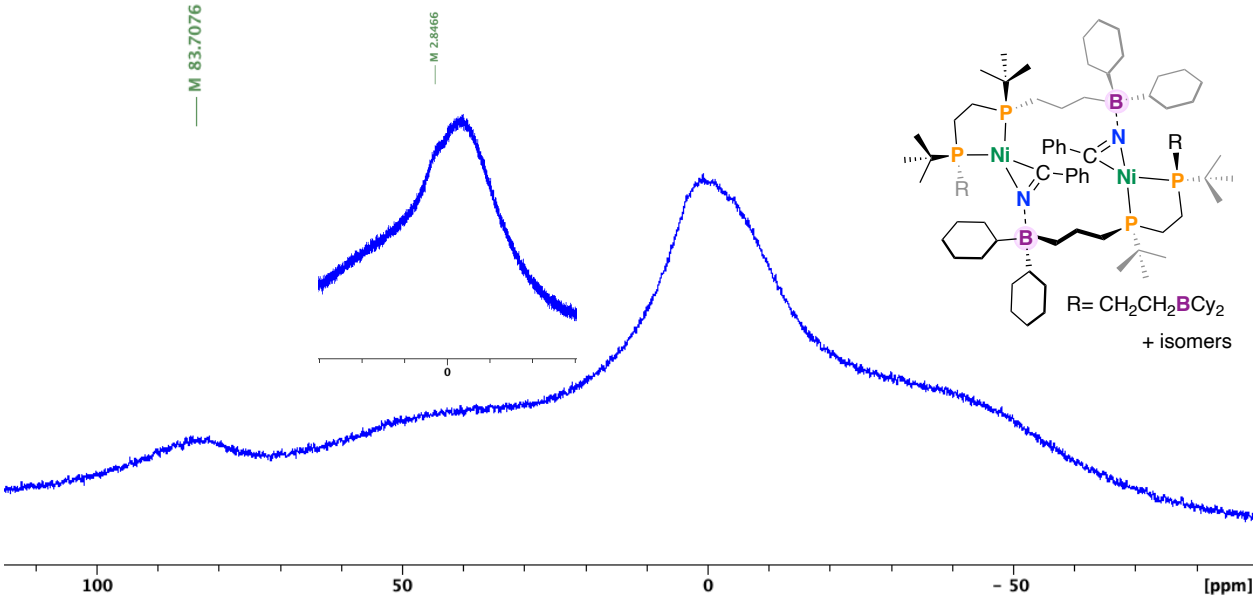

Figure S12. 3, $^{13}C\{^{1}H\}$ NMR, tol-d_8, 125 MHz, 298 K.

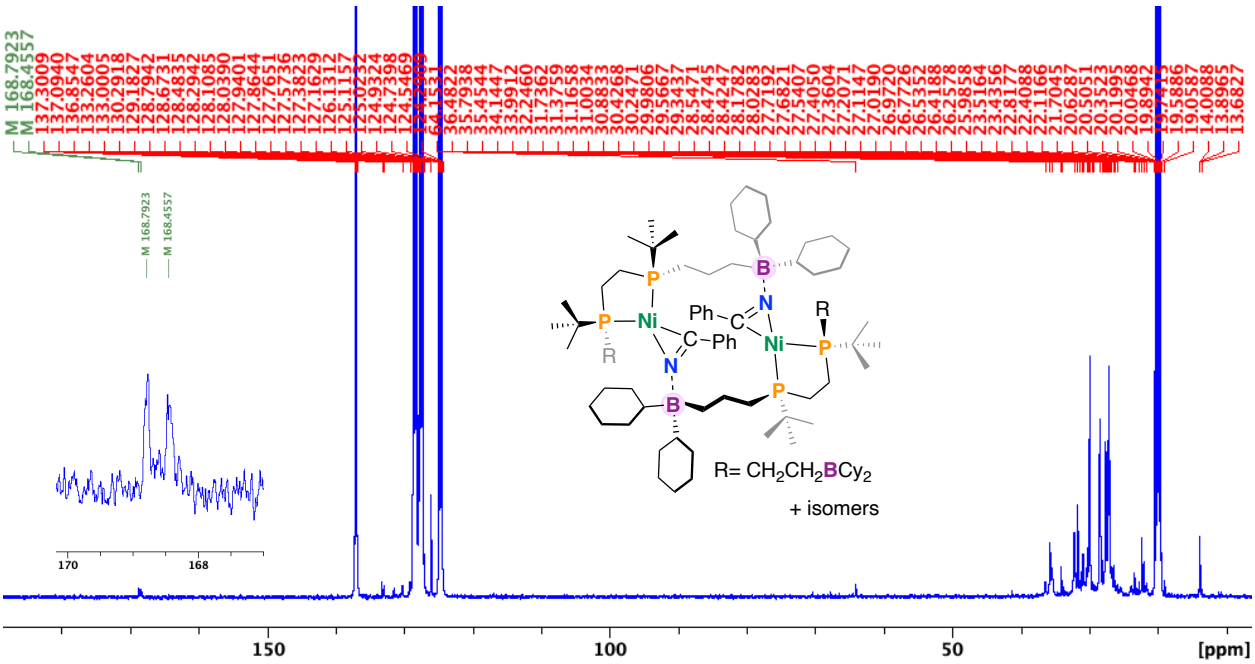

Figure S13. 3, IR Overlay of free PhCN and complex **3** comparing υ(CN).

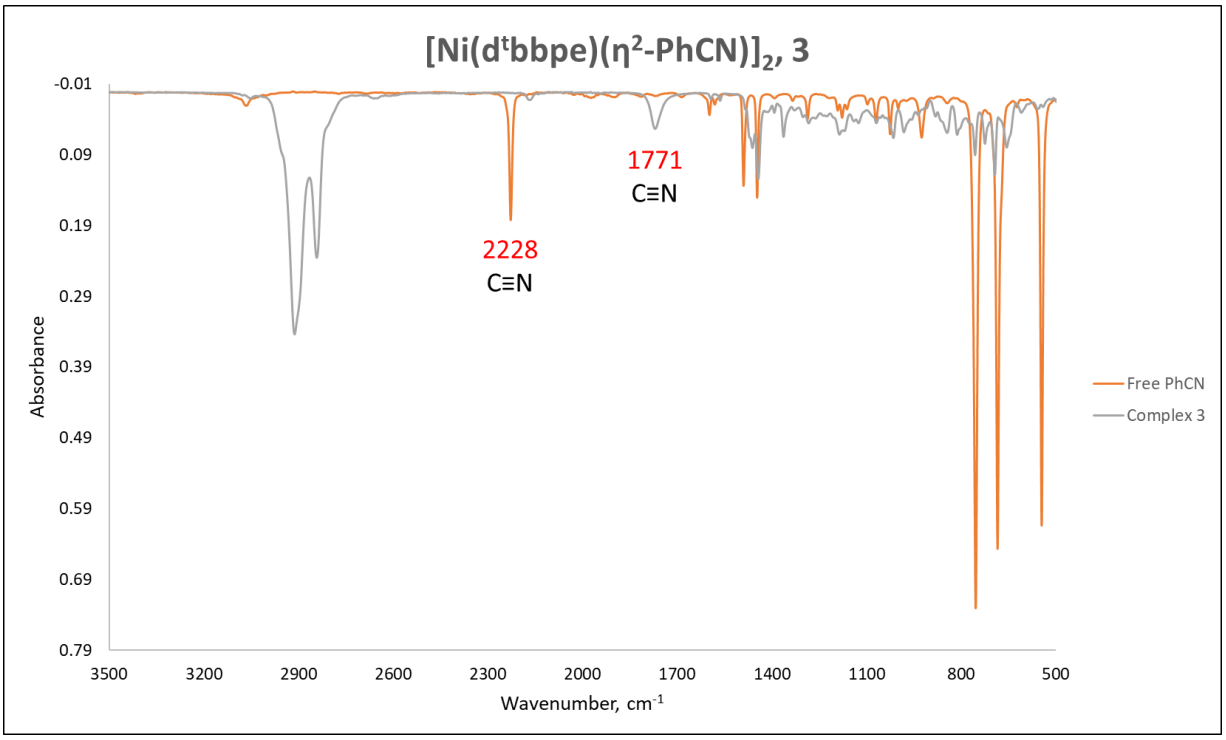

Figure S14. 4, ^{1}H NMR, tol-d$_8$, 500 MHz, 298 K (* = impurities).

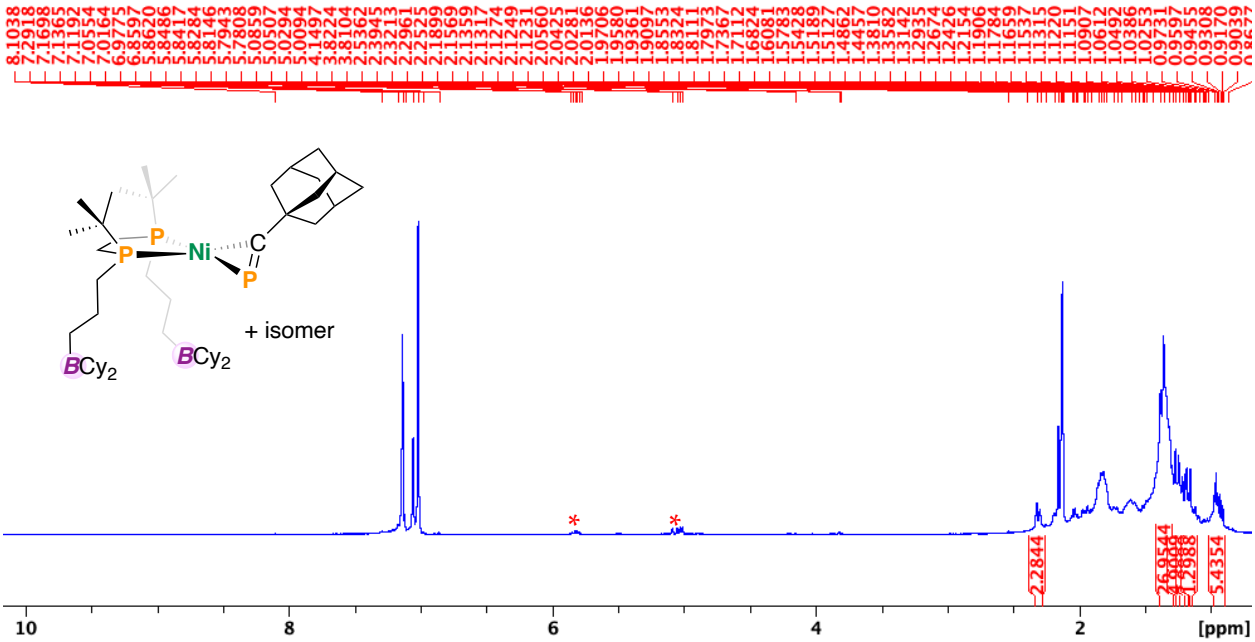

Figure S15. 4, ^{1}H -$^{1}H\{^{31}P\}$ NMR Overlay, tol-d_8, 500 MHz, 298 K.

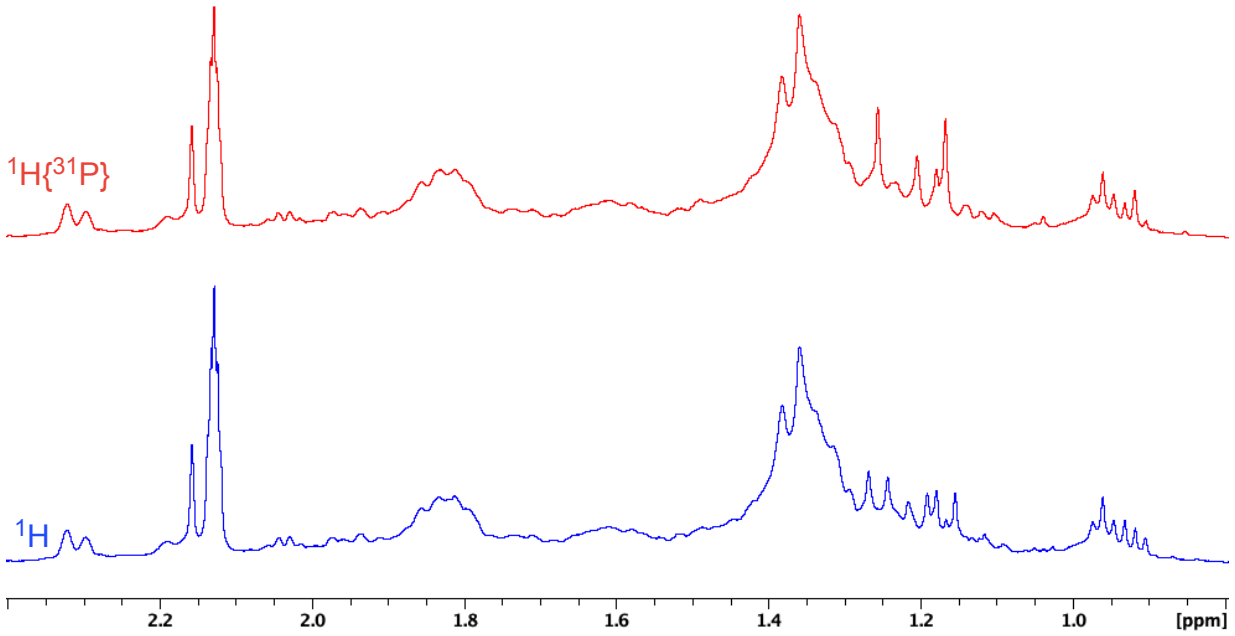

Figure S16. 4, $^{31}P\{^{1}H\}$ NMR, tol-d_8, 203 MHz, 298 K (* = 4% free ligand).

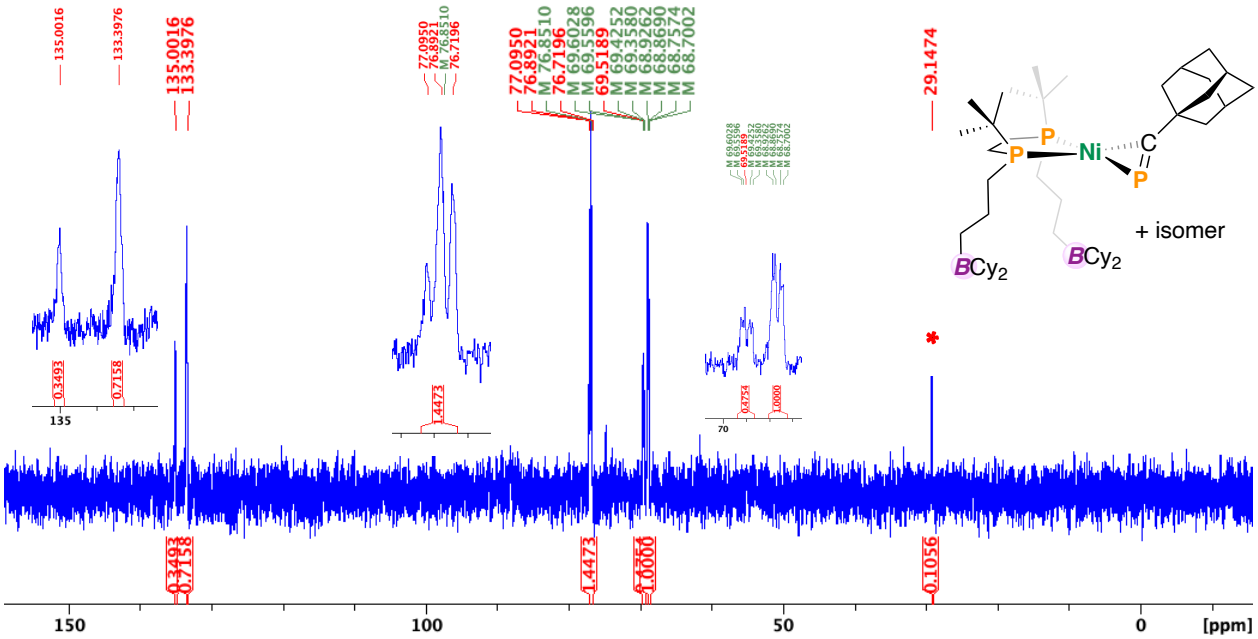

Figure S17. 4, $^{11}B\{^{1}H\}$ NMR, tol-d_8, 160.5 MHz, 298 K.

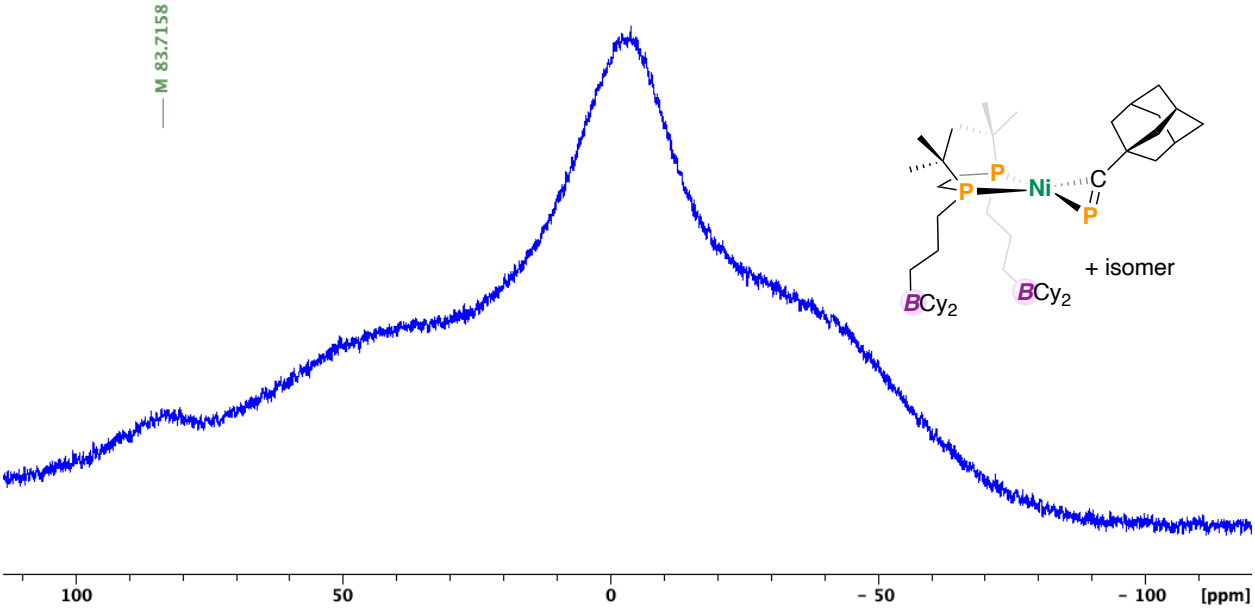

Figure S18. 4, $^{13}C\{^{1}H\}$ NMR, tol-d_8, 125 MHz, 298 K.

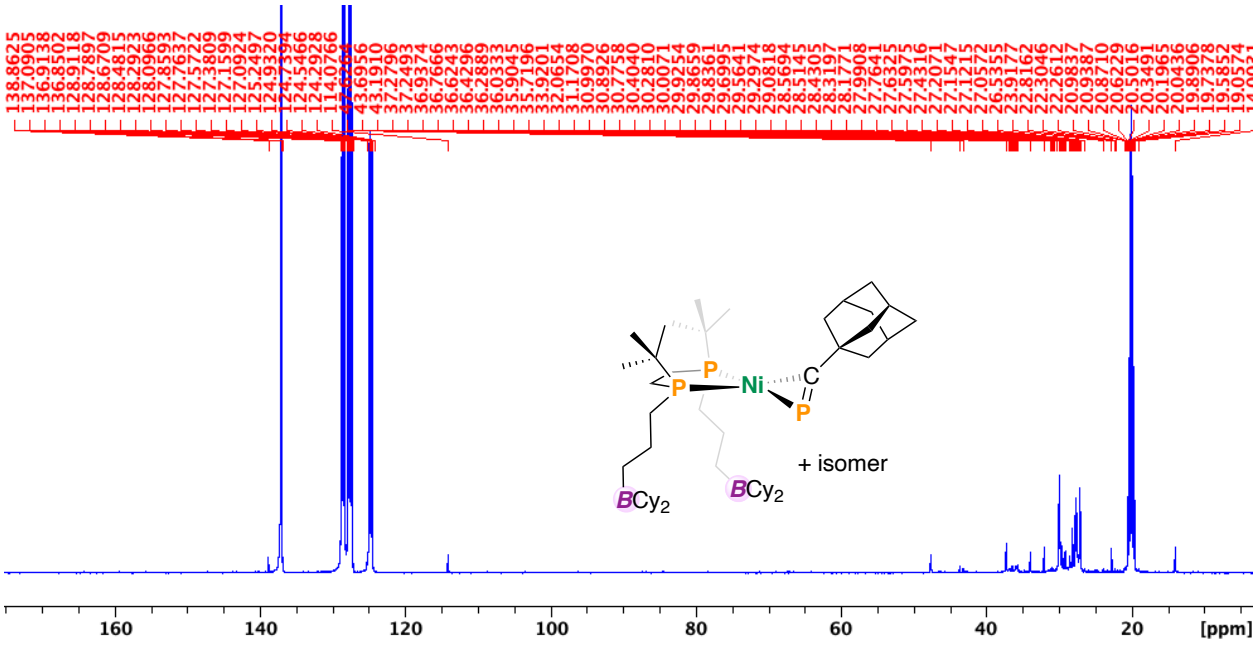

Figure S19. 4, ^{1}H-$^{13}C\{^{1}H\}$ HMBC NMR, tol-d_8, 125 MHz, 298 K.

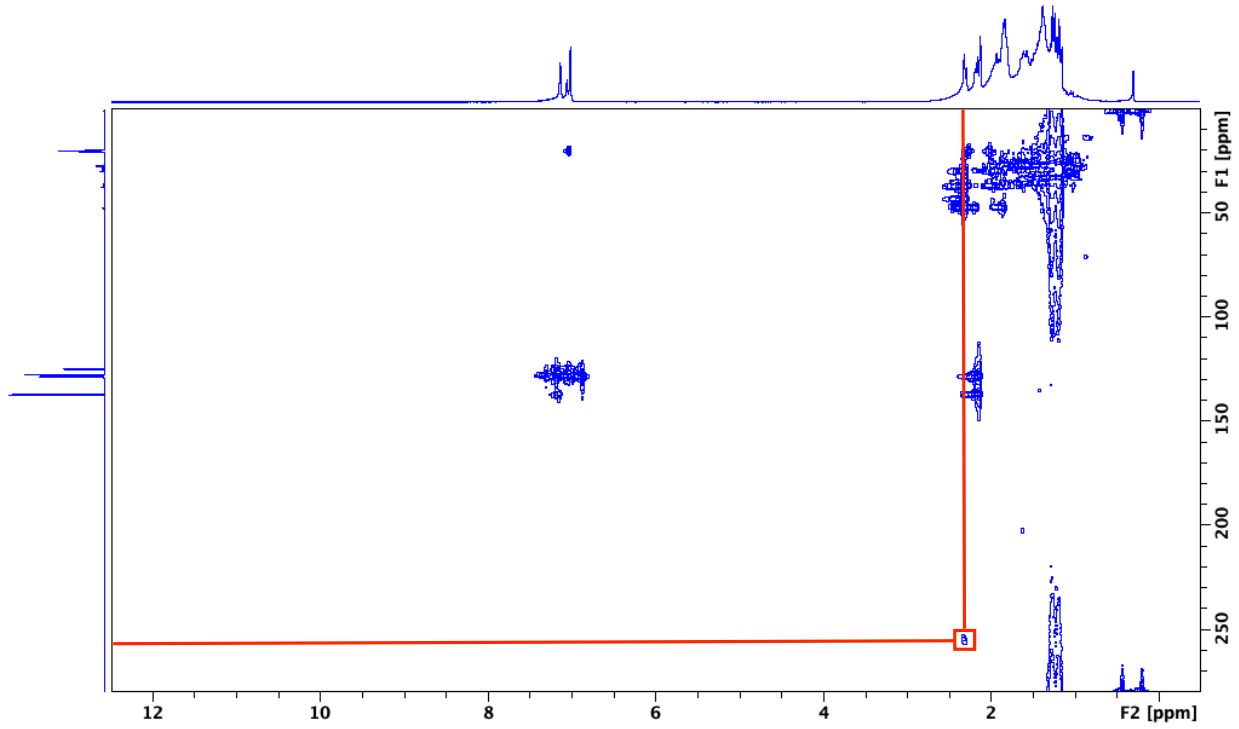

Figure S20. Reaction of **1** with 1-AdCN, $^{31}P\{^{1}H\}$ NMR, tol-d_8, 202.5 MHz, 298 K.

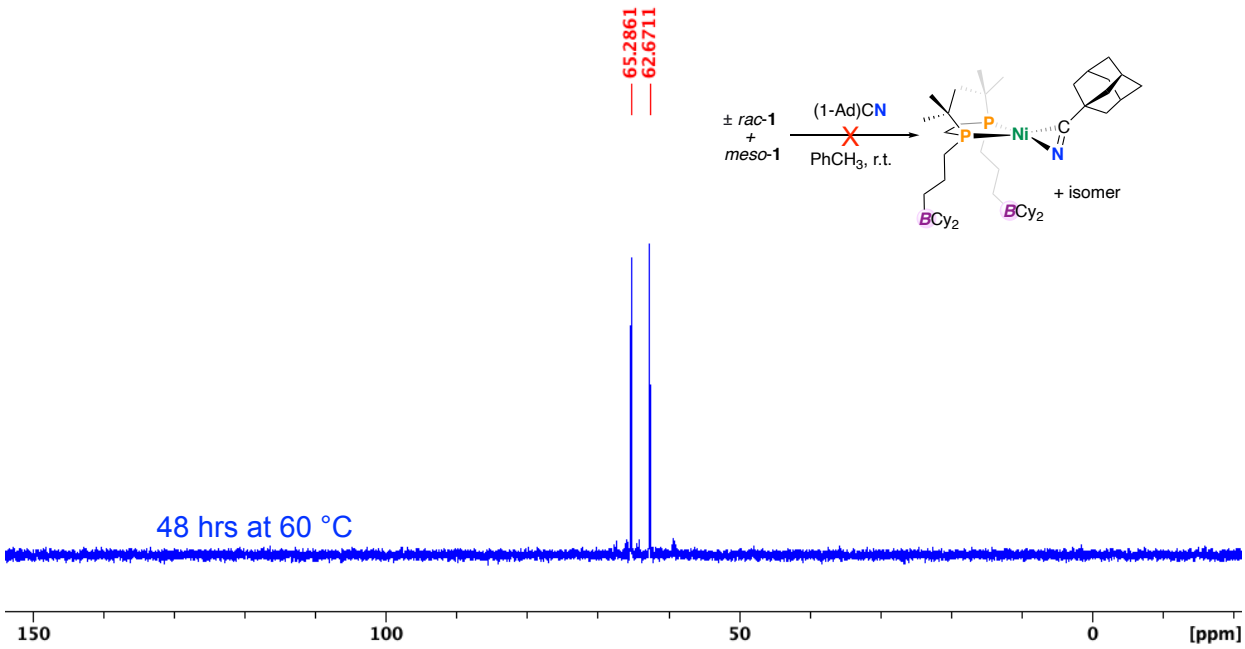

Catalytic Hydroboration Details.

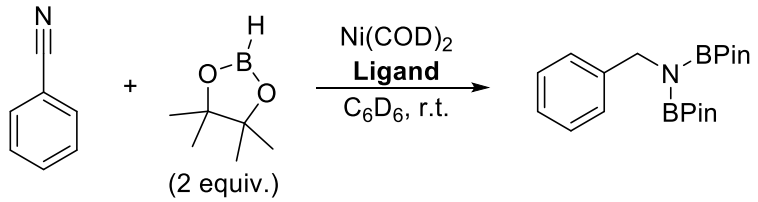

Representative Catalytic Procedure: To a J-Young NMR tube was added PhCN (0.014 g, 0.136 mmol), HBPin (0.044 g, 0.344 mmol), and HMDSO, as an internal standard, and dissolved in 0.4 mL C_6D_6. To the reaction mixture was added [$Ni(COD)_2$] (0.004 g, 0.015 mmmol) alongside t^tbbpe (0.010 g, 0.021 mmol). The reaction was monitored by $^{11}B\{^1H\}$ and ^1H NMR spectroscopy over 72 h.

Table S1: Reagent information for each catalytic run. %Yield determined by ^1H NMR spectroscopy utilizing HMDSO as an internal standard after approximately 72 h. Ligand acronyms: 1,2-bis(ditertbutylphosphino)ethane (d^tbpe), di-*tert*-butylboranyldiphosphinoethane (d^tbbpe), and tri-*tert*-butylboranyldiphosphinoethane (t^tbbpe).

Run	PhCN (g)	HBPin (g)	[$Ni(COD)_2$] (g)	Ligand	Ligand (g)	HMDSO (Amount)	% Yield
1	0.014	0.044	0.004	t^tbbpe	0.01	0.136 g	80
2	0.014	0.025	0.004	d^tbbpe	0.007	4 µL	40
3	0.017	0.062	0.004	d^tbpe	0.006	0.165 g	97
4	0.01	0.028	0.002	--		0.097	12
5	0.015	0.041	--	t^tbbpe	0.004	4 µL	7

Chart S1. Comparison of Ni(0) catalysts featuring boron in the secondary coordination sphere for the hydroboration of PhCN using HBPin.

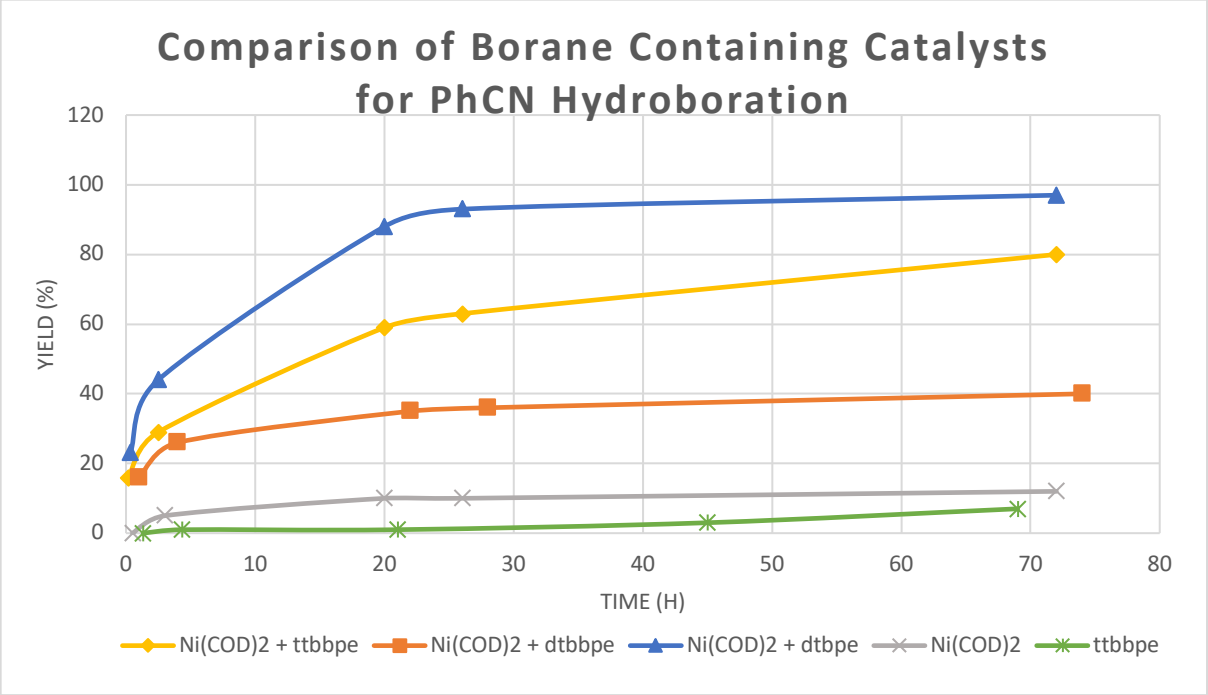

Table S2. Time and % Yield data for Chart 1. % Yield determined by ^{1}H NMR (C_6D_6, 500 MHz, 298K,) comparing to an internal HMDSO standard.

$Ni(COD)_2$ + t^tbbpe		$Ni(COD)_2$ + d^tbbpe		$Ni(COD)_2$ + d^tbpe		$Ni(COD)_2$		t^tbbpe	
Time	**Yield**	**Time**	**Yield**	**Time**	**Yield**	**Time**	**Yield**	**Time**	**Yield**
0.17	16	1	16	0.33	23	0.5	0	1.33	0
2.5	29	4	26	2.5	44	3	5	4.33	1
20	59	22	35	20	88	20	10	21	1
26	63	28	36	26	93	26	10	45	3
72	80	74	40	72	97	72	12	69	7

Table S3. TOF values.

Entry	$Ni(COD)_2$ + t^tbbpe	$Ni(COD)_2$ + d^tbbpe	$Ni(COD)_2$ + d^tbpe	$Ni(COD)_2$	t^tbbpe
TOF final (h^{-1})	0.11	0.05	0.15	0.022	0.012

Figure S21. Hydroborylation of PhCN using t^tbbpe, ^{1}H NMR (C_6D_6, 500 MHz, 298K). Product [$PhCH_2N(BPin)_2$] aromatic ortho-hydrogen resonance is highlighted in black.

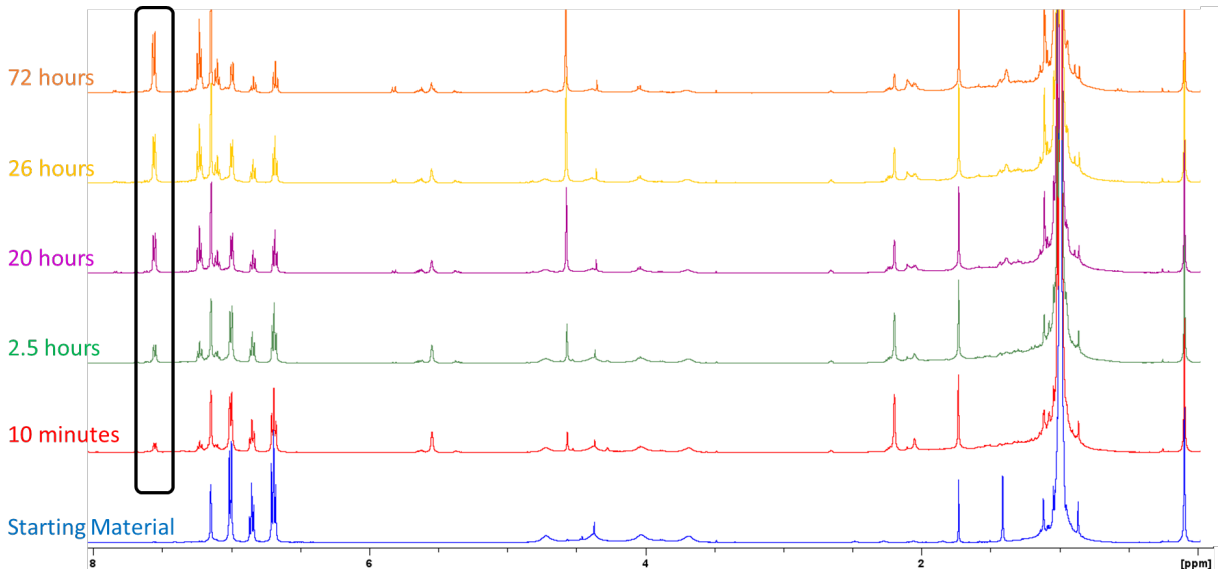

Figure S22. Hydroborylation of PhCN, $^{11}B\{^1H\}$ NMR (C_6D_6, 161 MHz, 298K). Product [$PhCH_2N(BPin)_2$] boron resonance is highlighted in black.

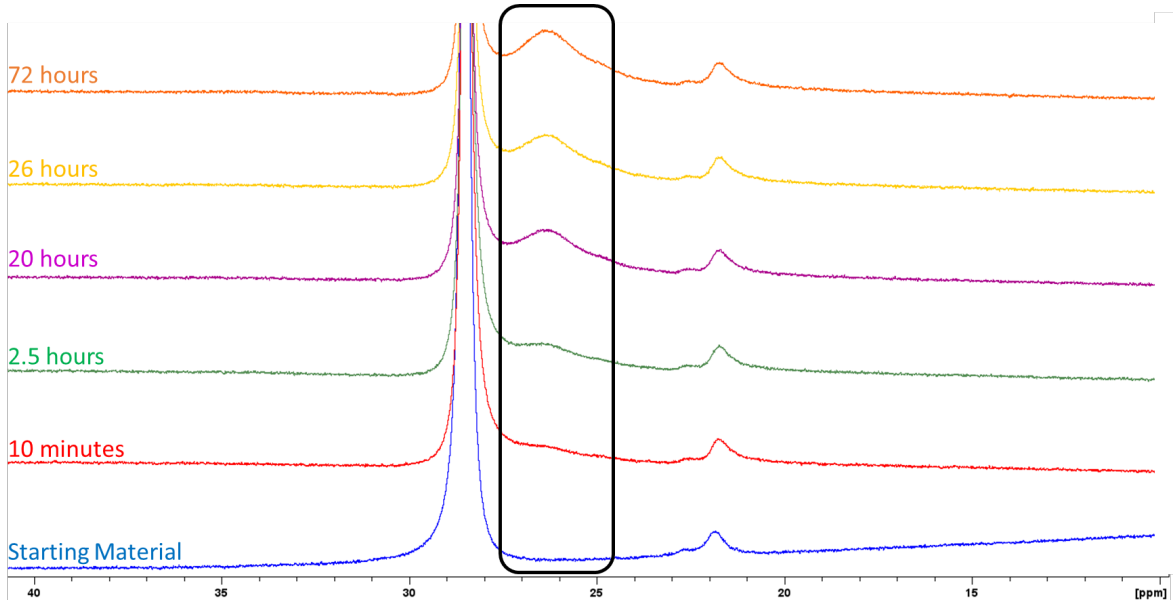

Crystallographic details.

Single crystal X-ray diffraction (scXRD) data for *meso*/*meso*-**2** was collected using a Bruker D8 Venture diffractometer equipped with an Apex detector and IμS Cu microsource at the University of Windsor. All crystals were mounted on a MiTeGen loop. Using Molybdenum K-α radiation (λ = 0.71 Å) at 170(2) K.

Cell refinement and data reduction were performed using Apex3.[1] An empirical absorption correction, based on the multiple measurements of equivalent reflections and merging of data was performed using SADABS.[2] Data conversion from XDS to SADABS file format was performed using XDS2SAD.[3] The space group was confirmed by XPREP.[4]

Routine checkCIF and structure factor analyses were performed using Platon.[5] CCDC **2251021** contains the supplementary crystallographic data for this paper. These data can be obtained free of charge from The Cambridge Crystallographic Data Centre *via* www.ccdc.cam.ac.uk/data_request/cif.

[1] Bruker (2016). APEX3, SAINT and SADABS. Bruker AXS Inc., Madison, Wisconsin, USA.

[2] L. Krause, R. Herbst-Irmer, G. M. Sheldrick, and D. Stalke, *J. Appl. Cryst.* **2015**, *48*, 3-10.

[3] XDS2SAD, G. M. Sheldrick, 2008, University of Gottingen, Germany.

[4] a) XPREP, **2014**, Bruker AXS Inc., Madison, Wisconsin, USA. b) XPREP Version 2008, G. M. Sheldrick, 2008 Bruker AXS Inc., Madison, Wisconsin, USA.

[5] A. L. Spek, *Acta Cryst*. **2009**, *D65*, 148.

Table S4. Crystallographic data for *meso*/*meso*-**2**.

Empirical formula	$C_{49}H_{89}B_2NNiP_2$
Formula weight	834.48
Temperature/K	170.0
Crystal system	Triclinic
Space group	*P-1*
a/Å	13.2771(17)
b/Å	13.8480(18)
c/Å	15.682(2)
α/°	67.397(5)
β/°	68.276(5)
γ/°	78.741(5)
Volume/Å^3	2468.0(6)
Z	2
ϱ_{calc}g/cm^3	1.123
μ/mm^{-1}	0.490
F(000)	916.0
Crystal size/mm^3	0.1 × 0.08 × 0.05
Radiation	MoKα (λ = 0.71073)
2Θ range for data collection/°	3.97 to 56.8
Index ranges	-17 ≤ h ≤ 17, -18 ≤ k ≤ 18, -20 ≤ l ≤ 20
Reflections collected	159104
Independent reflections	12337 [R_{int} = 0.0511, R_{sigma} = 0.0231]
Data/restraints/parameters	12337/0/504
Goodness-of-fit on F^2	1.110
Final R indexes [I>=2σ (I)]	R_1 = 0.0419, wR_2 = 0.1124
Final R indexes [all data]	R_1 = 0.0534, wR_2 = 0.1260
Largest diff. peak/hole / e Å^{-3}	1.03/-0.45

$R1 = \Sigma \, ||F_o|-|F_c|| \, / \, \Sigma \, |F_o|$; $wR2 = [\Sigma(w(F_o^2 - F_c^2)^2) / \Sigma \, w(F_o^2)^2]^{1/2}$

Computational Details.

All calculations were performed using version 4.2.1 of the ORCA computational package[6] and were run on the Graham cluster maintained by Compute Canada. All geometry optimizations and frequency calculations were performed at the BP86-D3(BJ)/def2-TZVP [7] level of theory. The RI approximation was used to enhance computational efficiency, along with the auxiliary basis *def2/J*[8]. Convergence criteria were met using *Grid4* and *FinalGrid6* integral grid sizes. Frequency calculations (*NumFreq*) were performed to confirm that each optimized geometry was a true minimum indicated by the absence of imaginary frequencies. Single-point calculations were performed at the BP86-D3(BJ)/def2-TZVP level of theory on optimized geometries using a Universal Solvation Model (*SMD*) to obtain thermochemical values in solvent. The solvent applied for all complexes was "TOLUENE".

Accurate electronic energies were determined using the "gold-standard" of quantum chemistry (CCSD(T)) at the DLPNO-CCSD(T)/def2-TZVP[9] level of theory. The RIJCOSX approximation was used to enhance computational efficiency, along with a *def2/J*[9] auxiliary basis set. As well, a *def2-TZVP/C*[10] auxiliary basis set was used.

To obtain accurate thermochemical information, the final Gibbs free energies for each chemical species were calculated using the following equation.

$$\Delta G_{solv} = E_{el}(DLPNO\text{-}CCSD(T)) + \Delta G_{correction}(DFT) + \Delta G^{\circ}_{solv}(DFT)$$

$E_{el}(DLPNO\text{-}CCSD(T))$ is the final electronic energy from a DLPNO-CCSD(T)/def2-TZVP calculation, $\Delta G_{correction}(DFT)$ is the $G\text{-}E_{el}$ (Gibbs free energy minus the electronic energy) from a BP86-D3(BJ)/def2-TZVP calculation, and $\Delta G^{\circ}_{solv}(DFT)$ is the sum of ΔG_{ENP}(*CPCM Dielectric)* and ΔG_{CDS}(*Free-energy(cav+disp))* from an *SMD* single point calculation.

[6] F. Neese, "Software update: the ORCA program system, version 4.0" WIREs *Comput. Mol. Sci.* 2017, e1327. DOI: 10.1002/wcms.1327

[7] a) S. Grimme, S. Ehrlich, L. Goerigk, *J. Comput. Chem.* 2011, ***32***, 1456; b) S. Grimme, J. Antony, S. Ehrlich, H. Krieg, *J. Chem. Phys.* 2010, ***132***, 154104; c) F. Weigend, R. Ahlrichs, *Phys. Chem. Chem. Phys.* 2005, ***7***, 3297.

[8] F. Weigend, *Phys. Chem. Chem. Phys.* 2006, ***8***, 1057.

[9] a) C. Riplinger, P. Pinski, U. Becker, E.F. Valeeve, F. Neese, *J. Chem. Phys.* 2016, ***144***, 024109; b) C. Riplinger, B. Sandhoefer, A. Hansen, F. Neese, *J. Chem. Phys.* 2013, ***139***, 134101; c) C. Riplinger, F. Neese, *J. Chem. Phys.* 2013, ***138***, 034106.

[10] A. Hellweg, C. Hattig, S. Hofener, W. Klopper, *Theor. Chim. Acta* 1990, ***77***, 123.

Figure S23. Potential Energy Surface scan (PES) for complex 4_intra